



# Silicon wet etching: Hillock formation mechanisms and dynamic scaling properties



D.A. Mirabella, G.P. Suárez, M.P. Suárez, C.M. Aldao\*

*Institute of Materials Science and Technology (INTEMA), University of Mar del Plata and National Research Council (CONICET),  
Juan B. Justo 4302, B7608FDQ Mar del Plata, Argentina*

## HIGHLIGHTS

- We studied the scaling properties of an etching model reproducing hillock patterns.
- We found that the model presents three distinctive regimes.
- Conventional and anomalous scaling was found depending on hillock apices stability.

## ARTICLE INFO

### Article history:

Received 13 April 2013  
Received in revised form 1 August 2013  
Available online 15 October 2013

### Keywords:

Scaling  
Etching models  
Monte Carlo simulations

## ABSTRACT

Surface roughening due to anisotropic wet etching of silicon was studied experimentally and modeled using the Monte Carlo method. Simulations were used to determine the consequences of site-dependent detachment probabilities on surface morphology for a one- and two-dimensional substrate models, focusing on the formation mechanisms of etch hillocks. Dynamic scaling properties of the 1D model were also studied. Resorting to the height–height correlation function and the structure factor, it is shown that the model presents conventional and anomalous scaling (faceted) depending on the stability of the hillocks tops. We also found that there is an intermediate regime that cannot be described by the Family–Vicsek or anomalous scaling ansatz.

© 2013 Elsevier B.V. All rights reserved.

## 1. Introduction

The miniaturization of electronic devices has been made possible by the production of microstructures with nanometer scale. Anisotropic or orientation-dependent wet chemical etching based on KOH is a common technique to manufacture microdevices. Si(100), is one of the most studied surfaces because of its relevance in semiconductor microelectronics. Wet chemical etching of Si(100) with aqueous KOH results in the appearance of inhomogeneities of pyramidal type (hillocks) [1–4].

In the past we derived a simple site-dependent etching model that reproduces the formation of pyramid hillocks in Si(100) [5,6]. In this model, pyramid apices etch slower than expected using simple bonding energetics, which has been attributed to a masking mechanism produced by an external agent or intrinsic surface properties [3,5]. This model predicts how the surface changes from a relatively smooth pattern in the absence of masking to a completely texturized (hillocked) one as pyramid tops are more stable. A morphology showing pyramids and relatively flat regions (valleys) between them emerges at intermediate values of the hillocks apices stability.

Surfaces that exhibit irregular geometries can be analyzed in terms of the scaling properties of the surface fluctuations [7]. The dynamical scaling behavior of a growing/etching surface with evolution arises from the competition between roughening and smoothing mechanisms. A large number of theoretical and experimental studies have helped in the understanding

\* Corresponding author. Tel.: +54 223 4816600; fax: +54 223 4810046.  
E-mail addresses: [cmaldao@mdp.edu.ar](mailto:cmaldao@mdp.edu.ar), [cmaldao@fi.mdp.edu.ar](mailto:cmaldao@fi.mdp.edu.ar) (C.M. Aldao).

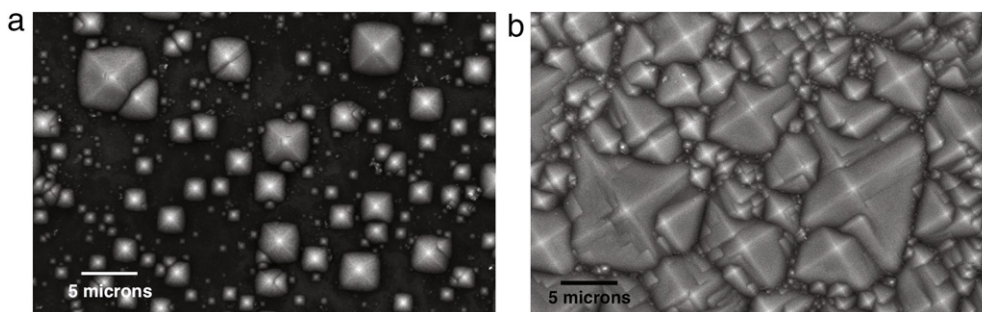


**Fig. 1.** (a) Hillocks and valleys on a Si(100) surface etched in 2 M KOH for 1 h at 60 °C. (b) Hillocks on a Si(100) surface etched in 0.3 M KOH for 1 h at 60 °C.

of possible mechanisms that generate surface roughness. Continuum and discrete growth models have provided scaling relations between roughness and time for a growing interface as well as the roughness dependence of the spatial scale of observation in the experiments. Surface structures that preserve a similar morphology upon a change of magnification are termed self-affine and obey the well-known Family–Vicsek (FV) scaling ansatz, which plays a central role in growth theories [8,9]. However, only a very small number of systems exhibit FV scaling. For instance, it has been reported that the formation of features during etching or the presence of grains in film growth leads to a more complex roughening process.

Motivated by these findings and following the work of Dotto and Kleinke [10,11] and more recently of Oliveira and Aarao Reis [12,13], we studied the dynamic scaling properties for a model that describes etching within a RSOS model. Different regimes that reflect the conventional scaling ansatz and anomalous scaling are obtained by simply varying the apex stability in our model. Also, a regime that cannot be described by the Family–Vicsek or anomalous scaling ansatz was also found.

## 2. Silicon wet etching

Silicon surfaces associated with growth and etching have been and continue to be of great interest as both processes are of technological relevance because of their role in the fabrication of microelectronic devices [1,14]. Silicon etching in aqueous solutions, such as KOH or  $\text{NH}_4\text{OH}$ , is widely used in producing a variety of devices by micromachining that requires the production of microstructures with nanometer precision. The formation of micropyramids that accompany Si(100) etching is a well-known phenomenon and an explanation for their appearance has been the goal of many investigations for years. Fig. 1 shows two SEM Si(100) surfaces after wet etching in 2 M and 0.3 M KOH solutions at 60 °C. Both systems are in steady state in the sense that further etching does not alter the statistical properties of the resulting surface characteristics. Surfaces exhibit a rough appearance with pyramidal hillocks of different sizes. However, the morphologies are very different, as the surface of Fig. 1(a) exhibits hillocks and relative flat regions, while no valleys are observed in Fig. 1(b).

The pyramid formation in Si(100) etching is a consequence of the high anisotropic dissolution ratios, with (100) and (110) surfaces dissolving much more rapidly than the (111) planes [3,5]. This leads to exposing the slower etching (111) planes that constitute the sides of pyramidal features. Thus, a restricted-solid-on-solid model (RSOS) is a good representation of the Si(100) etching [15]. Besides stable sides, for hillocks to form, their apices must be relatively resistant to etching as discussed in Ref. [16].

If etching at steps is much faster than at terraces and steps etch independently, step-flow etching predominates. This means that the crystal is etched by the continuous retreat of their steps. In this case, since terraces are rarely attacked, the surface morphology is dominated by step roughening that can be described with a one-dimensional substrate. Etching in vicinal Si(111) surfaces has been found to present these characteristics [17–19] with the formation of 2D hillocks. It is found that  $[\bar{1}\bar{1}2]$  steps sites are etched much faster than  $[11\bar{2}]$  step sites. When Si(111) miscut in the  $[\bar{1}\bar{1}2]$  direction is etched, a characteristic morphology appears. The etched step presents many straight step segments oriented in the  $[11\bar{2}]$  directions that constitute two-dimensional etch hillocks giving a shark's tooth shape to the structure [17]. This phenomenon can also be observed at the sides of the pyramids in Fig. 1(a), as they are vicinal (111) surfaces, and will be the subject of the present study.

## 3. Model and simulations

We performed simulations using the standard Monte Carlo method. The surface step is represented by a one-dimensional vector where each element corresponds to the height at each site. We adopted a restricted-solid-on-solid model (RSOS) in which particles are arranged such that the heights of neighboring columns can differ at most by only one particle to reproduce the step in a vicinal Si(111) surface. In our model, the substrate morphology is determined by the height of the columns relative to a flat reference surface.

During the simulation, a single site is chosen at random and the detachment event takes place with a probability that depends on the site coordination number. This is the only process that determines the final surface morphology. Other processes, such as rearrangement of surface particles (diffusion) or redeposition, are not allowed. Site specific etch rates were

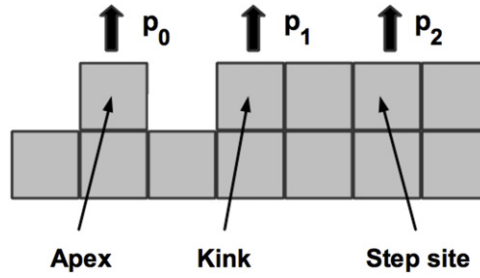


**Fig. 2.** Schematic for a one-dimensional substrate that describes the detachment probability of the three different types of sites.

chosen in order to produce hillocks. The simulation starts from a flat substrate configuration and evolves with successive annihilations of substrate particles until it approaches steady state. We checked that steady state was reached by assessing the evolution of the surface roughness.

Based on a model where only first neighbor interactions are considered, the parameters that determine the step morphology reduce to the etching rates of three distinct types of sites that can be related to the particle coordination number. Since we are dealing with a solid-on-solid model, all particles have at least one first neighbor at the bottom that has no effect in computing the site-specific etch rates. The etching probabilities will be referred as  $p_i$ , where  $i$  is the number of first neighbors excluding the bottom one. So we call sites with 0, 1 and 2 neighbors, apices, kinks, and step sites respectively, as shown in Fig. 2. For hillocks to form within a step, their tops must etch slower than it was expected from site bonding energetics. This is due by any of the masking mechanism discussed in Ref. [6] and it was taken into account by reducing the etching probability of apices. Kinks must be the fastest etching sites, and then a value of  $p_1 = 1$  was adopted for their detachment probability. Different values for  $p_2$  were explored to finally adopt 0.01 as hillocks of sound sizes formed. Results as a function of apex stability  $p_0$  will be reported. Monte Carlo simulations were carried out for arrays of different lengths; the results presented in this paper correspond to  $L = 512$  and  $L = 1000$ . We checked that the system was in steady state monitoring the roughness constancy with time. Thus, the results presented here correspond to different Monte Carlo times, from  $10^4$  for  $p_0 = 0.5$  to  $2 \times 10^6$  for  $p_0 = 0.05$ . Periodic boundary conditions were used to avoid edge effects.

#### 4. Dynamic scaling

Dynamic scaling is common framework to describe the interface fluctuations observed in growth and etching processes. Many of these interfaces in nature are examples of self-similar objects, and their growths exhibit nontrivial scaling properties that allow us to categorize them into universality classes [7]. The surface or interface width or roughness in 1D,  $W(t)$ , is defined as the rms deviation of the height field around its mean value:

$$W(L, t) = \sqrt{\frac{1}{L} \sum_{i=1}^L [h(i, t) - \bar{h}(t)]^2}, \quad (1)$$

where  $h(i, t)$  is the surface height measured from the flat substrate of size  $L$  at the position  $i$  at the time  $t$  and  $\bar{h}(t)$  is the mean height of the interface at the same time.  $W(L, t)$  increases with time as a power law,  $W(t) \sim t^\beta$ , for as long as the lateral correlation length,  $\zeta(t) \sim t^{1/z}$ , is smaller than the system size  $L$ . Since the correlation length  $\zeta(t)$  accounts for the spatial region of the system that has become correlated, the stationary regime is then reached when  $t_s \sim L^z$ . This means that the only characteristic scale length is the system size  $L$ . Thus, for longer times the roughness becomes a constant  $W \sim L^\alpha$ . This behavior is described by the so-called Family–Vicsek [10,11] dynamic scaling ansatz

$$W(L, t) \sim L^\alpha f(t/L^z), \quad (2)$$

$\alpha$ ,  $\beta$ , and  $z$  are the roughness, growth, and the dynamic scaling exponents, respectively, and characterize the spatial correlations of the interface, the roughness temporal evolution, and the coarsening process of the characteristic lateral correlation length of the interface.

Since experiments may not deal with temporal evolution of the growth process one can analyze only the final interface using other mathematical tools to compute scaling exponents. One of this is the height–height correlation function HHCF,  $C(l, t)$ , which is defined as

$$C(l, t) = \langle (h(x+l, t) - h(x, t))^2 \rangle^{1/2}, \quad (3)$$

where  $h(l, t)$  is the surface height at a distance  $l$  from a reference site and the averaging is done over distinct reference sites. For a self-affine surface,  $C(l, t)$  scales with  $l$  as

$$C(l, t) \approx l^f f(t/l^z) \quad (4)$$

where  $f \sim \text{constant}$  for  $L \gg l$ .

Another useful tool is the power spectrum (PS) or surface structure factor  $S(k, t)$  defined as

$$S(k, t) = \langle h(k, t)h(-k, t) \rangle, \quad (5)$$

being  $h(k, t)$  the  $k$ -th Fourier mode of the surface height deviation around its spatial average for a given time  $t$

$$h(k, t) = \frac{1}{L^{1/2}} \sum_x [h(x, t) - \bar{h}(t)] \exp(ikx). \quad (6)$$

The dynamic scaling hypothesis reflects into the structure factor as

$$S(k, t) = k^{-(2\alpha+1)} g(t/k^{-z}). \quad (7)$$

For  $u \ll 1$   $g(u) = u(2\alpha + 1)/z$  and for  $u \gg 1$   $g(u) = \text{constant}$ . Then:

$$\begin{aligned} S(k, t) &\sim k^{-(2\alpha+1)} & u \ll 1 \\ S(k, t) &\sim t^{(2\alpha+1)/z} & u \gg 1. \end{aligned} \quad (8)$$

However, some experimental observations deviate from the Family–Vicsek function, Eq. (2), and they have been proposed to present a new type of scaling, namely anomalous scaling (AS) [10,11,20,21]. The term AS refers to the observation that local and global surface fluctuations may have distinctly different scaling exponents. This leads to the existence of an independent local roughness exponent  $\alpha_{\text{loc}}$  that characterizes the local interface fluctuations and differs from the global roughness exponent  $\alpha$ . A new ansatz is needed to account for this new type of scaling. Thus, the local interface width

$$w(l, t) \sim \langle [h(x, t) - \bar{h}_l] \rangle_l^{1/2} \quad (9)$$

scales as

$$\begin{aligned} w(l, t) &\sim t^\beta, & \text{for } l^2 \ll t \ll L^2, & \text{ and} \\ w(l, t) &\sim l^{\alpha_{\text{loc}}} t^{\beta - \alpha_{\text{loc}}/z}, & \text{for } t \ll l^2, \end{aligned} \quad (10)$$

where  $\beta_{\text{loc}} = (\alpha - \alpha_{\text{loc}})/z$  is an anomalous growth exponent and  $l$  is the window size see, for example, Refs. [22,23]. From Eqs. (3) and (9),  $C(l, t)$  and  $w(l, t)$  can be easily related as  $C(l, t) \sim w(l, t)$ . In our work we used the HHCF for scaling analysis.

According to the work of López and co-workers [24,25], four different possible types of scaling can be distinguished,

$$\begin{aligned} \text{If } \alpha_s < 1 \Rightarrow \alpha_{\text{loc}} &= \alpha_s \begin{cases} \alpha_s = \alpha \Rightarrow \text{Family–Vicsek} \\ \alpha_s \neq \alpha \Rightarrow \text{intrinsic anomalous} \end{cases} \\ \text{If } \alpha_s > 1 \Rightarrow \alpha_{\text{loc}} &= 1 \begin{cases} \alpha_s = \alpha \Rightarrow \text{super-rough} \\ \alpha_s \neq \alpha \Rightarrow \text{faceted anomalous.} \end{cases} \end{aligned} \quad (11)$$

$\alpha$  is the global roughness exponent,  $\alpha_{\text{loc}}$  is the local roughness exponent obtained from HHCF, and  $\alpha_s$  the spectral roughness exponent deduced from the PS.

In our model, as hillocks appear, the surface loses its self-affinity and it is then expected that fluctuations at local and global scales differ, given rise to the appearance of anomalous scaling. Since also it is possible to control the hillock stability by simply varying the hillock apex etch rate, our model allows us to study how the dynamic scaling properties change as a function of the density of hillocks and their average size. Resorting to the HHCF and PS, we studied the scaling properties as the system changes from a smooth surface to a completely hillocked one.

## 5. Results and discussion

Slow-etching step sites and relatively stable hillock apices are needed for hillocks to form. Thus, kinks must be the fastest etching sites, and a value of 1 was adopted for their detachment probability. Step sites must be robust, and we explored different values for the detachment probability from them; the results presented here correspond to a probability  $p_2 = 0.01$ . Dynamic scaling exponents were obtained using Monte Carlo simulations varying the hillock apex stability  $p_0$ . Fig. 3 shows the etched profiles for several values of  $p_0$  with  $p_2 = 0.01$ . It is possible to identify three types of surface morphologies. The first one corresponds to  $p_0 > 0.2$ , where the etched step morphology is relatively straight with few scattered hillocks of very small size. As  $p_0$  is decreased ( $p_0 < 0.2$ ), the number of apices rapidly increases and hillocks start to be relevant. Thus, the resulting surface morphology presents small hillocks separated by flat regions that we call valleys. This morphology, in which hillocks form and coexist scattered on a surface of limited roughness, is regularly observed in silicon etching, as observed in Fig. 1(b), and we refer to it as pyramid-and-valley regime. As  $p_0$  is decreased even further hillocks become larger, as apices have a lower probability to be removed, while etching continues at the valleys reducing their size to eventually make them disappear given rise to a completely texturized surface.

We systematically studied how the dynamic scaling properties of the system change as  $p_0$  decreases. In Figs. 4–6 we show the plots of the HHCF and PS for three values of the parameter  $p_0$ , under steady-state condition, each one corresponding to the above mentioned morphology types for  $L = 512$ . As it can be seen, for  $p_0 = 0.5$  the surface morphology is relatively flat

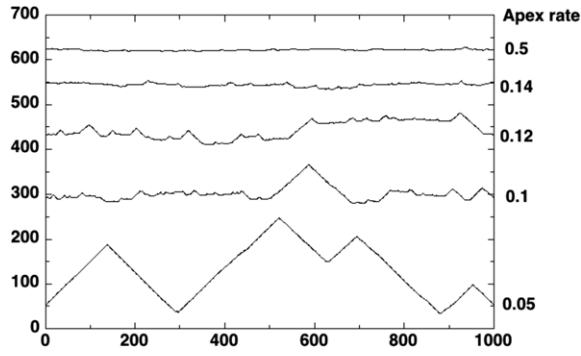


**Fig. 3.** Simulated etch morphologies of a one-dimensional substrate with different etch rates for apex sites. The etching rate for kinks is always equal to 1 and the etching rate for step sites is always equal to 0.01. Morphologies correspond to different Monte Carlo times, from  $10^4$  for  $p = 0.5$  to  $2 \times 10^6$  for  $p = 0.05$  to guarantee steady state.

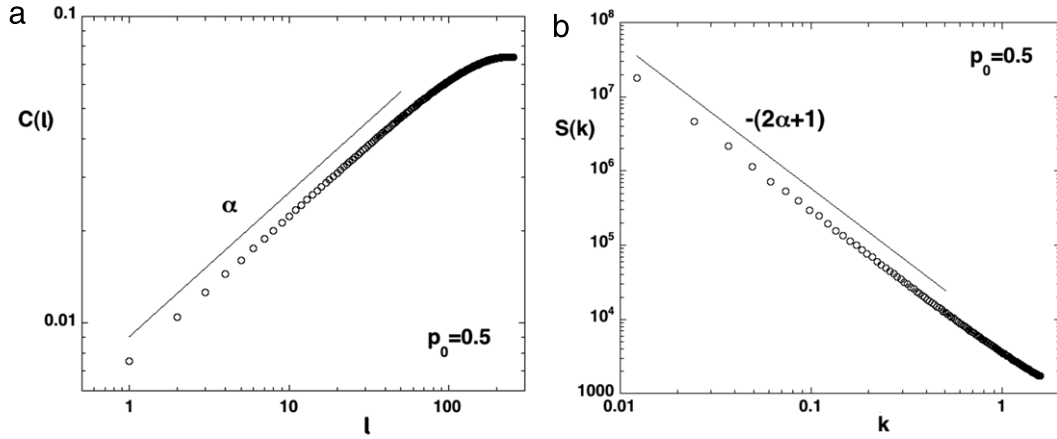


**Fig. 4.** (a) Height–height correlation function for  $p_2 = 0.01$  and  $p_0 = 0.5$ , the slope,  $\alpha$ , remains being close to that of the RSOS model ( $\alpha \approx 0.5$ ). (b) Power spectrum for  $p_2 = 0.01$  and  $p_0 = 0.5$ , the slope,  $2\alpha + 1 \approx 2$ , is consistent with the height–height correlation function ( $\alpha \approx 0.5$ ).

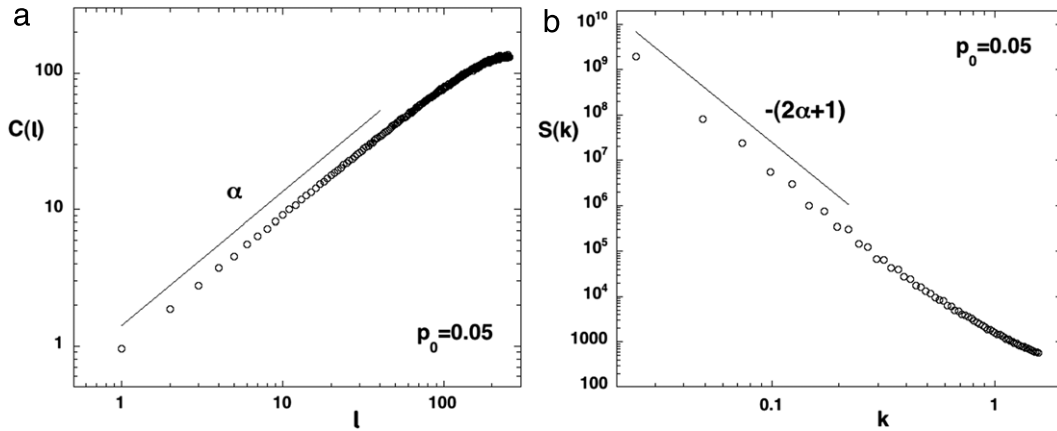


**Fig. 5.** (a) Height–height correlation function for  $p_2 = 0.01$  and  $p_0 = 0.05$ , the slope  $\alpha \approx 1$ . (b) Power spectrum for  $p_2 = 0.01$  and  $p_0 = 0.05$ , the slope  $2\alpha + 1 \approx 4$  implies  $\alpha \approx 1.5$ . Following Refs. [24,25], these results correspond to a faceted anomalous scaling.

with a few hillocks of very small size.  $C(l)$  and  $S(k)$  curves, Fig. 4(a) and (b) respectively, have a single slope and from them we obtain the same value of the roughness exponent  $\alpha_{loc} = \alpha_s = \alpha = 0.47$ . This value is very close to that expected for the Kim–Kosterlitz (KK) model ( $p_0 = p_1 = p_2 = 1$ )  $\alpha = 0.5$ . Despite the fact that  $p_2 = 0.01$ , very different from the value corresponding to the KK model, we checked that the change in the roughness exponent is due to the presence of apices as for  $p_0 = 1$  the roughness exponent recovers the KK value. Since  $\alpha_{loc} = \alpha_s = \alpha$  the system presents conventional scaling as predicted by Family–Vicsek ansatz of Eq. (2).

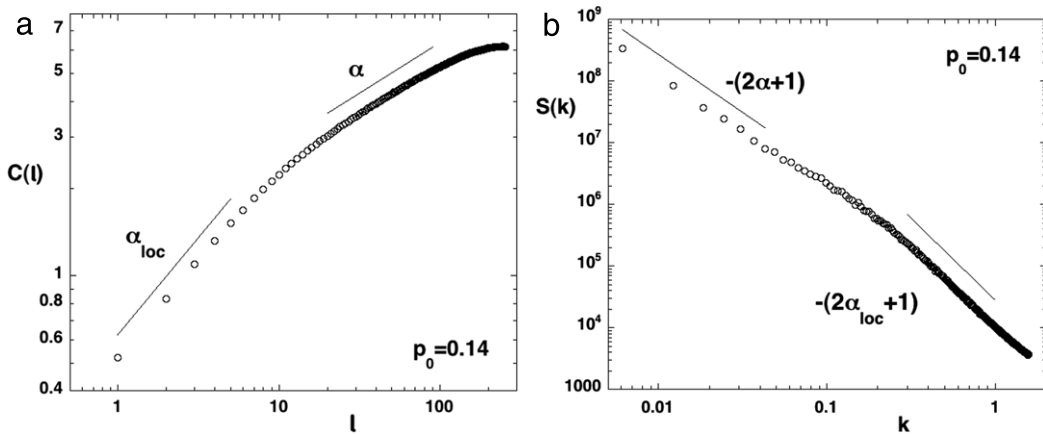


**Fig. 6.** (a) Height–height correlation function for  $p_2 = 0.01$  and  $p_0 = 0.14$ . Two values for the slope can be distinguished:  $\alpha_{loc} \approx 0.67$  and  $\alpha \approx 0.35$ . (b) Power spectrum for  $p_2 = 0.01$  and  $p_0 = 0.14$ . As for the height–height correlation function, two slopes can be distinguished:  $\alpha_{loc} \approx 0.81$  and  $\alpha \approx 0.35$ .

At the other extreme, for  $p_0 = 0.05$  where the system is almost completely texturized, both functions have a single slope but different values  $\alpha_{loc} = 0.98$  and  $\alpha_s = 1.49$ . This discrepancy between the values of the roughness exponent measured using HHCF ( $\alpha_{loc}$ ) Fig. 5(a) and PS ( $\alpha_s$ ) Fig. 5(b) fits with a class of anomalous scaling initially termed as super-roughening ( $\alpha_s > 1 \rightarrow \alpha_{loc} = 1$  and  $\alpha_s = \alpha$  [24,25]). In our model, as  $p_0 \rightarrow 0$ , we measured  $\alpha_{loc} \rightarrow 1$ , consistent with the results of Ref. [12]. This is expected for a surface completely covered with hillocks with no valleys in between because  $\alpha_{loc}$  measures the slope of the hillock sides, which is 1 for a perfect hillock under the RSOS condition. On the other hand, we also found that  $\alpha_s \rightarrow 1.5$  for  $p_0 \rightarrow 0$ . Interestingly, the Fourier transform of a triangular pulse goes as  $k^{-4}$ , which following Eq. (8), implies  $\alpha_s = 1.5$ . The small differences between the limit values of  $\alpha_s$  and  $\alpha_{loc}$  with those obtained for  $p_0 = 0.05$  can be attributed to the presence of small valleys and that the hillock slopes are not perfect, as seen in Fig. 3 in 1D and in Fig. 1(b) in 2D. Using the anomalous scaling (AS) classification proposed in Ref. [25], these findings correspond to a faceted AS. In Ref. [23], the hillock morphology can be obtained using the KPZ model but the thermal noise is replaced by a quenched columnar disorder whereas in our model, the observed faceting is consequence of local site-dependent etching since we only included thermal noise.

For  $p_0 = 0.14$ ,  $C(l)$  and  $S(k)$  clearly show two slopes Fig. 6(a) and (b) respectively. These results indicate that the FV ansatz as well as the AS are not adequate to describe the scaling behavior of the roughening in this type of behavior. Roughness exponents obtained by HHCF and the PS present two different slopes which are not consistent with the FV or the AS ansatz. Using the HHCF, at large distances the slope is 0.35 and at short distances the slope is 0.67, whereas using the PS they are 0.35 and 0.81, respectively. We correlate these findings with those obtained in Refs. [10–13] where the presence of two slopes can be associated with the appearance of a substructure such as grains of other type of features (hillock-and-valley in our model) and the crossover length at which the slope changes is related to their average size.

## 6. Conclusions

We analyzed a simple etching model, in which the only process present is the removal of particles. The model is a one-dimensional-RSOS reflecting the high stability of  $[11\bar{2}]$  steps sites in Si(111) vicinal surface. We found that varying the hillock apices stability the dynamic scaling properties of the system changes from conventional to faceted anomalous scaling. In passing from one type of scaling to the other one, there is an intermediate regime for which the currently scaling ansatz cannot be applied to describe it. In this regime, the presence of a more than one slope in the HHCF and PS correlates with the appearance of hillocks.

## Acknowledgments

This work was supported by the National Council for Scientific and Technical Research of Argentina (CONICET) and the University of Mar del Plata (Argentina).

## References

- [1] M. Elwenspoek, H. Jansen, *Silicon Micromachining*, Cambridge University Press, Cambridge, 1998.
- [2] Y. Jiang, Q. Huang, A physical model for silicon anisotropic chemical etching, *Semicond. Sci. Technol.* 20 (2005) 524–531.
- [3] D. Cheng, M.A. Gosálves, T. Hori, K. Sato, M. Shikida, Improvement in smoothness of anisotropically etched silicon surfaces: effects of surfactant and TMAH concentrations, *Sensors Actuators A* 125 (2006) 415–421.
- [4] R.A. Wind, M.A. Hines, Macroscopic etch anisotropies and microscopic reaction mechanisms: a micromachined structure for the rapid assay of etchant anisotropy, *Surf. Sci.* 460 (2000) 21–38.



- [5] M.P. Suárez, D.A. Mirabella, C.M. Aldao, Formation of pyramidal etch hillocks in a Kossel crystal, *Surf. Sci.* 599 (2005) 221–229.
- [6] D.A. Mirabella, M.P. Suárez, C.M. Aldao, Basic mechanisms for hillock formation during etching, *Physica A* 387 (2008) 1957.
- [7] A.-L. Barabási, H.E. Stanley, *Fractal Concepts in Surface Growth*, Cambridge University Press, Cambridge, 1995.
- [8] F. Family, T. Vicsek, Scaling of the active zone in the Eden process on percolation networks and the ballistic deposition model, *J. Phys. A* 18 (1985) L75–L81.
- [9] F. Family, T. Vicsek, *Dynamics of Fractal Surfaces*, World Scientific, Singapore, 1991.
- [10] M.E.R. Dotto, M.U. Kleinke, Kinetic roughening in etched Si, *Physica A* 295 (2001) 149–157.
- [11] M.E.R. Dotto, M.U. Kleinke, Scaling laws in etched Si surfaces, *Phys. Rev. B* 65 (2002) 245323.
- [12] T.J. Oliveira, F.D.A. Araao Reis, Effects of grains' features in surface roughness scaling, *J. Appl. Phys.* 101 (2007) 063507.
- [13] T.J. Oliveira, F.D.A. Araao Reis, Roughness exponents and grain shapes, *Phys. Rev. E* 83 (2011) 041608.
- [14] Z. Zhang, M. Lagally, *Morphological Organization in Epitaxial Growth and Removal*, in: *Series on Directions in Condensed Matter Physics*, vol. 14, World Scientific, Singapore, 1998.
- [15] D.A. Mirabella, M.P. Suárez, C.M. Aldao, Understanding the hillock-and-valley pattern formation after etching in steady state, *Surf. Sci.* 602 (2008) 1572.
- [16] M.A. Gosálves, R.M. Nieminen, Surface morphology during anisotropic wet chemical etching of crystalline silicon, *New J. Phys.* 5 (2003) 100.
- [17] J. Flidr, Y. Huang, M.A. Hines, An atomistic mechanism for the production of two- and three-dimensional etch hillocks on Si(111) surfaces, *J. Chem. Phys.* 111 (1999) 6970–6981.
- [18] J. Flidr, Y. Huang, T.A. Newton, M.A. Hines, Extracting site-specific reaction rates from steady state surface morphologies: kinetic Monte Carlo simulations of aqueous Si(111) etching, *J. Chem. Phys.* 108 (1998) 5542–5553.
- [19] T.A. Newton, Y. Huang, L.A. Lepak, M.A. Hines, The site-specific reactivity of isopropanol in aqueous silicon etching: controlling morphology with surface chemistry, *J. Chem. Phys.* 111 (1999) 9125–9128.
- [20] S. Huo, W. Schwarzscher, Anomalous scaling of the surface width during Cu electrodeposition, *Phys. Rev. Lett.* 86 (2001) 256–259.
- [21] A.E. Lita, J.E. Sanchez, Effects of grain growth on dynamic surface scaling during the deposition of Al polycrystalline thin films, *Phys. Rev. B* 61 (2000) 7692–7699.
- [22] N.-E. Lee, D.G. Cahill, J.E. Greene, Surface roughening during low-temperature Si epitaxial growth on singular vs vicinal Si(001) substrates, *Phys. Rev. B* 53 (1996) 7876–7879.
- [23] M. Kardar, Dynamic scaling phenomena in growth processes, *Physica B* 221 (1996) 60–64.
- [24] J.J. Ramasco, J.M. López, M.A. Rodríguez, Generic dynamic scaling in kinetic roughening, *Phys. Rev. Lett.* 84 (2000) 2199–2202.
- [25] I.G. Szendro, J.M. López, M.A. Rodríguez, Localization in disordered media, anomalous roughening, and coarsening dynamics of faceted surfaces, *Phys. Rev. E* 76 (2007) 011603.